METHODS FOR MONITORING LOCALITIES BASED ON REMOTE SENSING IMAGES. CASE STUDY: DUMBRAVITA, TIMIS COUNTY

E. ANGHEL, M. NICOLA, D. VUCULESCU, M. V. HERBEI, F. SALA
Banat University of Agricultural Sciences and Veterinary Medicine "King Michael I of Romania" from Timisoara, Timisoara, 300645, Romania
Corresponding author: florin_sala@usab-tm.ro

Abstract. *The study aimed to analyze and characterize an urban area based on satellite imagery. UAT Dumbravita, Timis County, Romania, was studied under the aspect of the variation of NDBI and NDVI indices. It was considered a period of four years, 2017 - 2020, for the study, and as the period of the year the summer season was taken into account. Satellite scenes, Landsat 8, were used, taken in July - August during the study period. Based on spectral information and established formulas, NDBI and NDVI indices were calculated. Data sets of 21011 were analyzed for each index calculated and year of study. The series of values of the two indices studied (NDBI, NDVI) presented statistical distributions of histogram type - normal fit. The ANOVA test evaluated and confirmed the data safety and the presence of the variance in the data series (F>Fcrit, p<0.001). According to the Diversity profile, NDVI presented a higher variation in 2020 and a lower one in 2018. Intermediate values were recorded for 2017 and 2019. The variation of NDVI index values in relation to NDBI during the study period was described by 2nd order polynomial equations for 2017 and 2018 in statistical safety conditions (R^2 = 0.729, p <0.001 , F = 28287 for 2017; R^2 = 0.773, p <0.001 F = 35695 for 2018). In the conditions of 2019 and 2020, the NDVI variation in relation to NDBI was best described by linear equations, in conditions of statistical safety (R^2 = 0.716, p <0.001, F = 53038 for 2019; R^2 = 0.798, p < 0.001, F = 83229 for the year 2020). The general analysis over the study period, mean values of NDBI and NDVI indices, led to a spline model, which most appropriately described, and in statistical safety, the NDVI variation relative to NDBI.*

Keywords*: NDBI, NDVI, monitoring, spline model, periurban area*

INTRODUCTION

In the study of terrestrial, natural, cultivated or urban areas, methods based on remote sensing offer a series of facilities based on spectral information and specific indices (GOVEDARICA et al., 2015; AL-BILBISI, 2019; POPESCU et al., 2020; CAO et al., 2021; DHARMAWAN et al., 2021).

Specific study techniques have been developed, based on remote sensing, in relation to the satellite system, spectral bands, image resolution, processing techniques, and the objectives pursued (ROY et al., 2017; BABAEIAN et al., 2019; JI et al., 2019; LIU et al., 2020; ZHANG et al., 2021a).

Various appropriate indices have been used to capture the spatial and temporal variability of urban ecosystems and to facilitate the quantification of aspects (HERBEI and SALA, 2020; LYNCH et al., 2020; ABUTALEB et al., 2021), or for the biomonitoring of urban habitats (DATCU et al., 2017).

Urban areas were studied in relation to elements of urban planning (WELLMANN et al., 2020), urban development (ZHANG et al., 2021b), spatial location / mapping urban areas (XIA et al., 2019), changes of urban landscape (ODINDI et al., 2012; KADHIM et al., 2016), ecological aspects (QIAN et al., 2020; DAI et al., 2021), green spaces (Huang et al., 2018), buildings and road infrastructure (AL-RUZOUQ et al., 2017; OTUOZE et al., 2021), heat islands and discomfort (HERBEI and SALA, 2020; ZHAO et al., 2020), pollution aspects (ZHOU et al., 2018; LINAG and PENG, 2020).

The present study aimed at analyzing and evaluating an urban hair area based on

satellite images, through specific remote sensing techniques, in relation to two major categories, urban buildings and the vegetation status.

MATERIAL AND METHODS

The study aimed to analyze and evaluate a peri-urban area using techniques based on remote sensing. UAT Dumbravita, Timis County, Romania was studied. Satellite scenes were used, Landsat 8.

The images were taken during the summer season, July - August, between 2017 and 2020. Based on satellite images, the NDBI (ZHA et al., 2003) relation (1), and NDVI (ROUSE et al., 1974) relation (2) indices were calculated.

$$NDBI = (\mathrm{SWIR} - \mathrm{NIR}) / (\mathrm{SWIR} + \mathrm{NIR}) \quad (1)$$

$$NDVI = \frac{NIR - R}{NIR + R} = (B5 - B4) / (B5 + B4) \quad (2)$$

The NDBI index uses the NIR and SWIR spectral bands to highlight constructed areas. This index highlights urban areas where there is usually a higher reflectance in the short-wave infrared (SWIR) region compared to the near-infrared (NIR) region. Applications include land use planning forecasts.

The NDVI index is a standardized index that allows an image to be generated that shows the areas covered by vegetation, also known as relative biomass. This index takes advantage of the contrast of the characteristics between two bands in a multispectral raster data set - the absorption of the chlorophyll pigment in the red band and the high reflectivity of the plant material in the near infrared band (NIR).

The data set was analyzed in terms of the frequency of distribution of values (histogram, diversity profile). The interdependence of the studied indices, NDVI in relation to NDBI, was analyzed on the complete data series, independently for each year of study, by regression analysis (R^2, p, F were used as statistical safety parameters).

The variation of NDVI in relation to NDBI, average values over the study period, was evaluated by statistical analysis ($\bar{\varepsilon}$ as a statistical safety parameter). he EXCEL calculation module and PAST software were used for data processing and analysis (HAMMER et al., 2001).

RESULTS AND DISCUSSIONS

The analysis of satellite images led to the values of the indices taken into account (NDBI and NDVI) during the four years of study, the summer season (July - August), in order to characterize the area under study.

The graphical distribution of the variation of the indices is shown in figure 1, with the representation of the safety interval and of the outlier values.

The graphical representation of the indices in the form of maps is shown in Figures 2 and 3. From the statistical analysis of the set of values considered for each index (21011 data), a normal distribution of values was found, Figure 4 a, b.

The ANOVA test evaluated and confirmed the data safety and the presence of the variance in the data series ($F > F_{crit}$, $p < 0.001$).

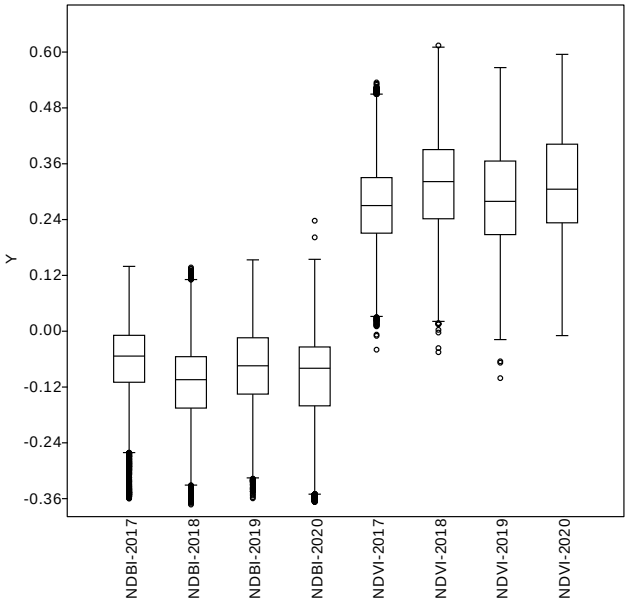

Fig. 1. Distribution of index values studied in Box plot format (with Outliers representation)

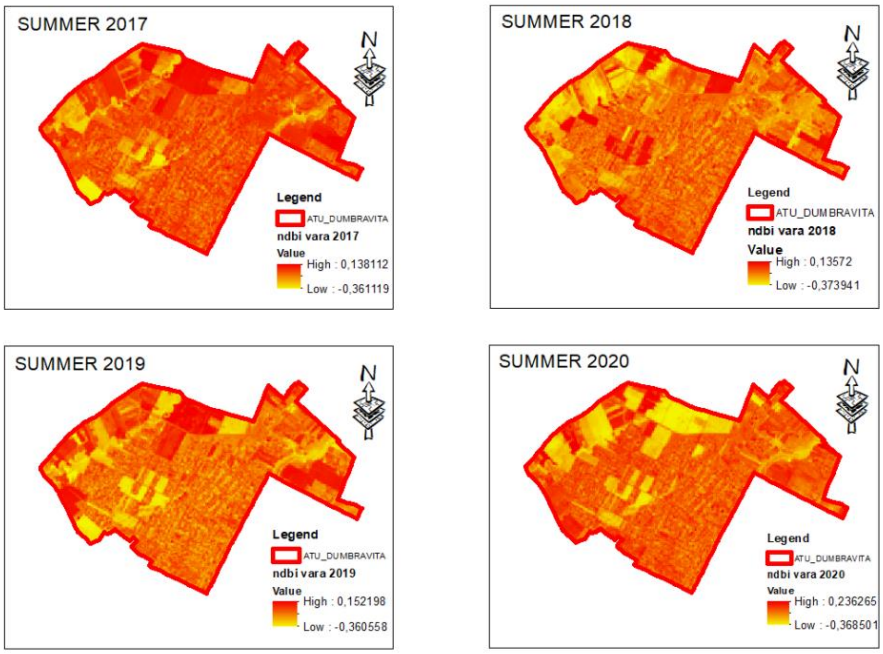

Fig, 2. NDBI map for the study period

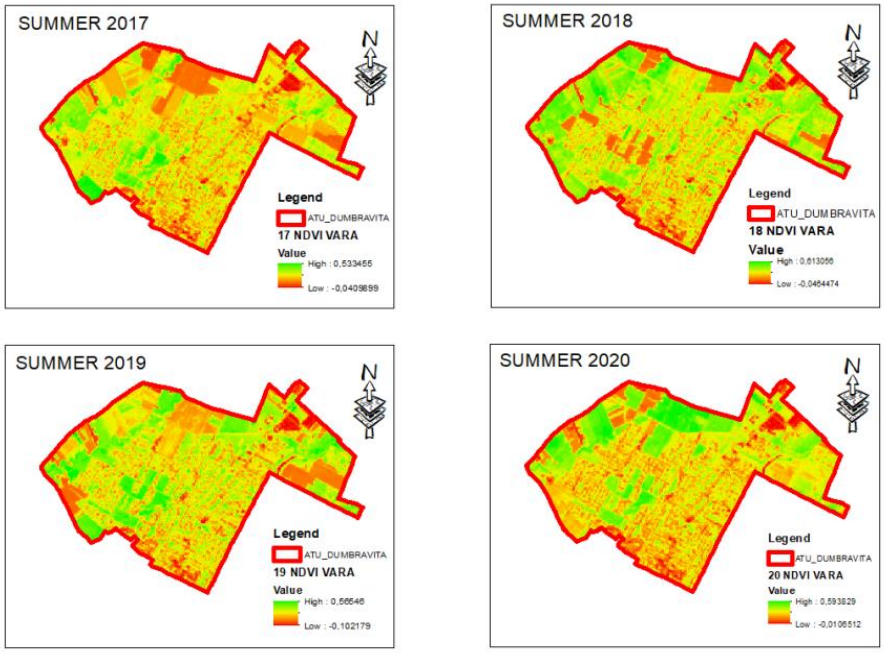

Fig. 3. NDVI map for the study period

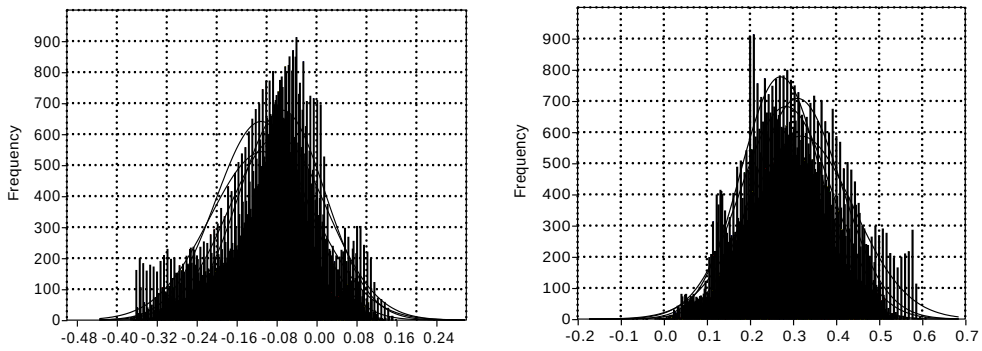

a) NDBI – Histogram reprezentation b) NDVI – Histogram reprezentation

Fig. 4. Histograms of data distribution for NDBI and NDVI indices for the studied area, period 2017 - 2020

According to the Diversity profile, NDVI presented a higher variation in 2020 and a lower one in 2018. Intermediate values were recorded for 2017 and 2019, figure 5.

The variation of the NDVI index values was analyzed in relation to the NDBI index for each year of the studied period. It was found that polynomial equations of degree 2 described the NDVI variation in relation to NDBI in the case of 2017 (example in figure 6) and 2018, respectively linear equations described the NDVI variation in relation to NDBI in the case of 2019 and 2020 (example in figure 7), in conditions of statistical uncertainty, table 1.

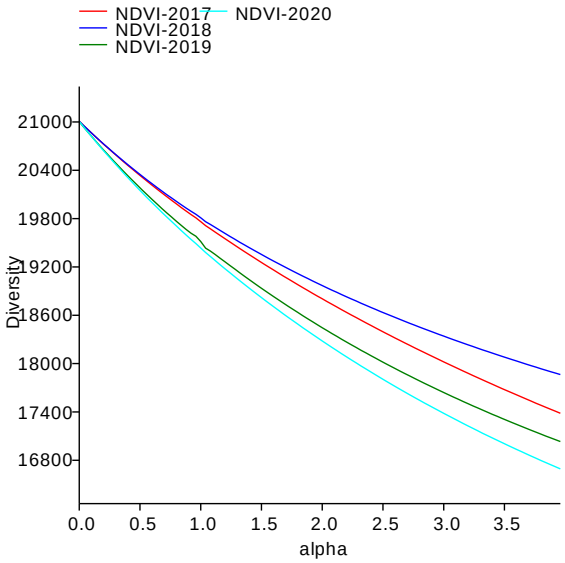

Fig. 5. Diversity profile for NDVI values

Table 1

Equations and statistical safety parameters for NDVI variation in relation to NDBI for the studied area

Year	Ecuation	Eq. No.	R^2	p	F
2017	$NDVI = -0.4358\,x^2 - 1.014\,x + 0.2069$	(3)	0.729	<0.001	28287
2018	$NDVI = -0.2846\,x^2 - 1.053\,x + 0.1999$	(4)	0.773	<0.001	35695
2019	$NDVI = -0.9104\,x + 0.2133$	(5)	0.716	<0.001	53038
2020	$NDVI = -1.028\,x + 0.2082$	(6)	0.798	<0.001	83229

x – NDBI values in studied years

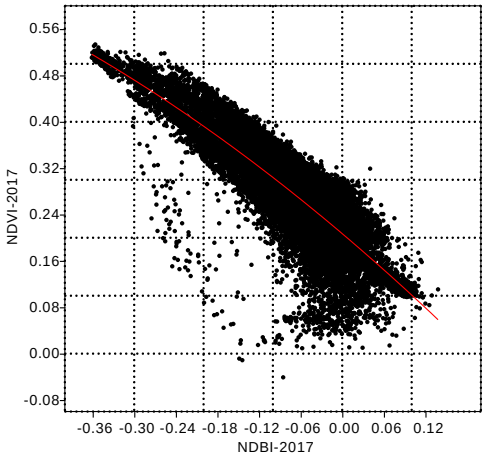

Fig. 6. Graphical representation of NDVI variation in relation to NDBI, year 2017

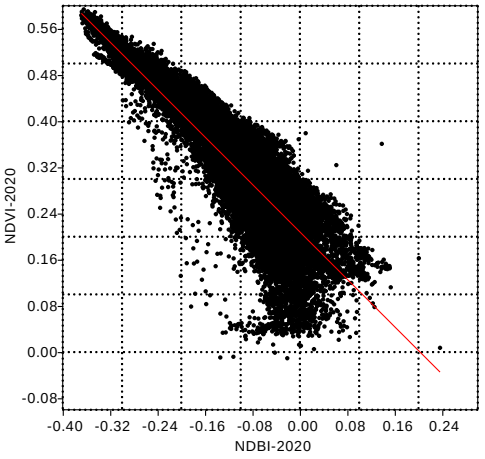

Fig. 7.Graphical representation of NDVI variation in relation to NDBI, year 2020

The analysis of the NDVI variation in relation to NDBI during the study period, average values, was best described by a spline model, the values obtained being presented in table 2. The graphical distribution of the spline model and the real values are represented in figure 8.

Table 2

Statistical values from the spline model

Trial image capture / year / NDBI			NDVI			
No	Year	x_i	y_i	ys_i	e_i	$I_{i/1}$
1	2017	-0.06851	0.27118	0.27104	-0.00052	1.000000
2	2018	-0.11093	0.31089	0.31379	0.00933	1.157726
3	2019	-0.07763	0.28397	0.28452	0.00194	1.049734
4	2020	-0.10719	0.31837	0.31505	-0.01043	1.162375

$\bar{\varepsilon} = 8.01\,\mathrm{E}-05$

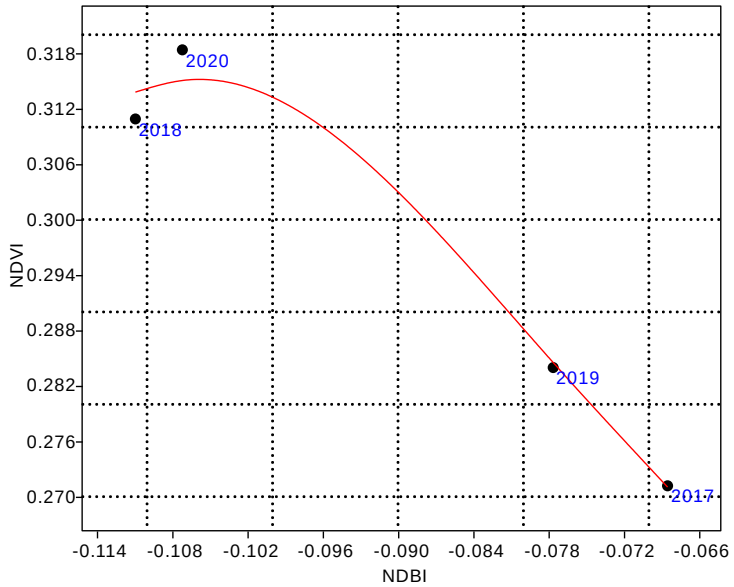

Fig. 8. Graphical representation of the real NDVI values and of the spline model regarding the NDVI variation in relation to NDBI for the studied area

CONCLUSIONS

The annual variation of the NDVI index in relation to NDBI for the area of Dumbravita locality, Timis county, was described by polynomial equations of degree 2 in the case of 2017 and 2018, respectively by linear functions in the case of 2019 and 2020.

The variation of the mean values of the NDVI index in relation to the NDBI during the study period was described by the spline model, in statistical safety conditions.

High values of the NDVI index were recorded in 2020, and shakes in 2017, in accordance with the variation of the NDBI index.

ACKNOWLEDGEMENT

The authors thanks to the GEOMATICS Research Laboratory, BUASMV "King Michael I of Romania" from Timisoara, for the facility of the software use for this study.

BIBLIOGRAPHY

ABUTALEB, K., MUDEDE, M.F., NKONGOLO, N., NEWETE, S.W. 2021. Estimating urban greenness index using remote sensing data: A case study of an affluent vs poor suburbs in the city of Johannesburg. The Egyptian Journal of Remote Sensing and Space Science, 24(3), Part1: 343-351.

AL-RUZOUQ, R., HAMAD, K., SHANABLEH, A., KHALIL, M. 2017. Infrastructure growth assessment of urban areas based on multi-temporal satellite images and linear features. Annals of GIS, 23(3): 183-201.

AL-BILBISI, H. 2019. Spatial Monitoring of Urban Expansion Using Satellite Remote Sensing Images: A Case Study of Amman City, Jordan. Sustainability, 11: 2260.

BABAEIAN, E., SIDIKE, P., NEWCOMB, M.S., MAIMAITIJIANG, M., WHITE, S.A., DEMIEVILLE, J., WARD, R.W., SADEGHI, M., LEBAUER, D.S., JONES, S.B., SAGAN, V., TULLER, M. 2019. A new optical remote sensing technique for high-resolution mapping of soil moisture. Frontiers in Big Data, 2: 37.

CAO, X., SHI, Y., ZHOU, L. 2021. Research on urban carrying capacity based on multisource data fusion - A case study of Shanghai. Remote Sensing, 13(14): 2695.

DAI, X., JOHNSON, B.A., LUO, P., YANG, K., DONG, L., WANG, Q., LIU, C., LI, N., LU, H., MA, L., YANG, Z., YAO, Y. 2021. Estimation of urban ecosystem services value: A case study of Chengdu, Southwestern China. Remote Sensing, 13(2): 207.

DATCU, A.-D., SALA, F., IANOVICI, N. 2017. Studies regarding some morphometric and biomass allocation parameters in the urban habitat on *Plantago major*. Research Journal of Agricultural Science, 49(4): 96-102.

DHARMAWAN, I.A., RAHADIANTO, M., HENRY, E., ENDYANA, C., AUFARISTAMA, M. 2021. Application of high-resolution remote-sensing data for land use land cover mapping of university campus. The Scientific World Journal, 2021: 5519011.

GOVEDARICA, M., RISTIC, A., HERBEI M.V., SALA, F. 2015. Object oriented image analysis in remote sensing of forest and vineyard areas. Bulletin UASVM Horticulture, 72(2): 362-370.

HERBEI, M.V., SALA, F. 2020. Evaluation of urban areas by remote sensing methods in relation to climatic conditions: Case study city of Timisoara. Carpathian Journal of Earth and Environmental Sciences, 15(2): 327-337.

HAMMER, Ø., HARPER, D.A.T., RYAN, P.D. 2001. PAST: Paleontological statistics software package for education and data analysis. Palaeontologia Electronica, 4(1): 1-9.

HUANG, C., YANG, J., JIANG, P. 2018. Assessing impacts of urban form on landscape structure of urban green spaces in China using Landsat images based on Google Earth Engine. Remote Sensing, 10(10): 1569.

JI, C., LI, X., WEI, H., LI, S. 2019. Comparison of different multispectral sensors for photosynthetic and Non-Photosynthetic Vegetation-Fraction Retrieval. Remote Sensing, 12: 115.

KADHIM, N., MOURSHED, M., BRAY, M. 2016. Advances in remote sensing applications for urban sustainability. Euro-Mediterranean Journal for Environmental Integration, 1: 7.

LIANG, L., GONG, P. 2020. Urban and air pollution: a multi-city study of long-term effects of urban landscape patterns on air quality trends. Scientific Reports 10: 18618.

LIU, M., YU, T., GU, X., SUN, Z., YANG, J., ZHANG, Z., MI, X., CAO, W., LI, J. 2020. The impact of spatial resolution on the classification of vegetation types in highly fragmented planting areas based on Unmanned Aerial Vehicle Hyperspectral Images. Remote Sensing, 12(1): 146.

LYNCH, P., BLESIUS, L., HINES, E. 2020. Classification of urban area using multispectral indices for urban planning. Remote Sensing, 12(15): 2503.

ODINDI, J., MHANGARA, P., KAKEMBO, V. 2012. Remote sensing land-cover change in Port Elizabeth during South Africa's democratic transition. South African Journal of Science, 108(5-

6): 60-66.

OTUOZE, S.H., HUNT, D.V.L., JEFFERSON, I. 2021. Monitoring spatial-temporal transition dynamics of transport infrastructure space in urban growth phenomena: A case study of Lagos - Nigeria. Frontiers in Future Transportation, 2: 673110.

POPESCU, C.A., HERBEI, M.V., SALA, F. 2020. Remote sensing in the analysis and characterization of spatial variability of the territory. A study case in Timis county, Romania. Scientific Papers Series Management, Economic Engineering in Agriculture and Rural Development, 20(1): 505-514.

QIAN, Y., ZHOU, W., PICKETT, S.T.A., YU W., XIONG D., WANG W., JING C. 2020. Integrating structure and function: mapping the hierarchical spatial heterogeneity of urban landscapes. Ecological Processes 9: 59.

ROUSE, J.W., HAAS, R.H., SCHELL, J.A., DEERING, D.W. Monitoring vegetation systems in the great plains with ERTS. In: Proceedings third Earth Resources Technology Satellite-1 Symposium, Greenbelt 1974, NASA SP–351(1), 3010-3017.

ROY, P.S., BEHERA, M.D., SRIVASTAV, S.K. 2017. Satellite Remote Sensing: Sensors, Applications and Techniques. Proceedings of the National Academy of Sciences, India, Section A - Physical Sciences 87: 465-472.

WELLMANN, T., LAUSCH, A., ANDERSSON, E., KNAPP, S., CORTINOVIS, C., JACHE, J., SCHEUER, S., KREMER, P., MASCARENHAS, A., KRAEMER, R., HAASE, A., SCHUG, F., HAASE, D. 2020. Remote sensing in urban planning: Contributions towards ecologically sound policies? Landscape and Urban Planning, 204: 103921.

XIA, N., CHENG, L., LI, M.C. 2019. Mapping urban areas using a combination of remote sensing and geolocation data. Remote Sensing, 11: 1470.

ZHA, Y., GAO, J., NI, S. 2003. Use of Normalized Difference Built-Up Index in automatically mapping urban areas from TM imagery. International Journal of Remote Sensing, 24(3): 583-594.

ZHANG, L., DONG, R., YUAN, S., LI, W., ZHENG, J., FU, H. 2021a. Making low-resolution satellite images reborn: A deep learning approach for super-resolution building extraction. Remote Sensing, 13(15): 2872.

ZHANG, Y., ZHAO, L., ZHAO, H., GAO, X. 2021b. Urban development trend analysis and spatial simulation based on time series remote sensing data: A case study of Jinan, China. PLoS ONE, 16(10): e0257776.

ZHAO, H., ZHANG, H., MIAO, C., YE, X., MIN, M. 2020. Linking heat source–sink landscape patterns with analysis of urban heat islands: Study on the fast-growing Zhengzhou City in Central China. Remote Sensing, 12(18): 2965.

ZHOU, C., LI, S., WANG, S. 2018. Examining the impacts of urban form on air pollution in developing countries: A case study of China's Megacities. International Journal of Environmental Research and Public Health, 15(8): 1565.